Chapter-3

Synthesis and Properties of Organotrialkoxysilane Functionalized Palladium-Cobalt Heterogeneous Catalysts for Oxygen Evolution Reaction

3.1 Introduction

Global energy demand has grown due to the direct use of fossil fuels and the rising industrialization of the world. Furthermore, the daily burning of fossil fuels emits vast amounts of greenhouse gases, contributing to global warming. In this aspect, electrochemical energy conversion is an excellent technique for replacing fossil fuel resources. In this regard, electrochemical water splitting is an essential strategy for producing clean and ecologically friendly energy (Ling et al.,2017). Although the electrochemical splitting of water has been known since the 19th century, when Paets van Troostwijk/Deiman and Nicholson/Carlisle produced one of the most fascinating scientific discoveries ever, revealing that electricity can disintegrate water into hydrogen and oxygen. The anodic process of water electrolyzers known as the oxygen evolution reaction (OER) is still a mystery (Fabbri et al 2014).

The mechanism of the reaction and the optimum catalyst in terms of activity and stability have not yet been identified. The OER is therefore surrounded by many unanswered questions and formidable obstacles. The creation of a highly active, reliable, and affordable electrocatalyst is urgently needed in order to hasten the market penetration of water electrolyzers. The OER mechanism on metal oxides has traditionally been drawn

from that on metal catalysts, where overpotential is the primary factor controlling the reaction. according to the Sabatier principle, the oxygen's ability to attach to the catalyst surface. The best catalyst, in terms of showing the least amount of overpotential, binds oxygen on its surface in a balanced manner(Viswanathan et al 2012; Man et al 2011) Two half-cell processes involved in electrochemical water splitting are the hydrogen evolution reaction (HER) and the oxygen evolution reaction (OER)(Gerken et al 2011). The OER takes place at the anode, while the HER takes place at the cathode. The total reaction requires a typical value of 1.23 V potential to be driven electrochemically. Because of the multistep electron transfer involving several high-energy intermediates, OER is the slower of the two half-cell reactions. Furthermore, OER is more straightforward to perform in an alkaline medium than an acidic one (Jiao et al 2015). Because of the abundance of protons in an acidic medium, HER is more superficial than in an alkaline medium. The pH of the electrolyte heavily influences the entire reaction of OER and HER. OER is a four electron-proton coupled reaction while HER is only a two electron-transfer reaction, and hence it can be easily expected that OER requires a higher energy (higher overpotential) to overcome the kinetic barrier of OER to occur. In the past several decades, the electrocatalytic OER has been extensively studied and various catalysts have been designed to improve electrode kinetics and stability under different electrolyte environments.

Noble metal-based catalysts, such as IrO_2 and RuO_2, have vigorous catalytic activity for OER, allowing for faster kinetics and higher efficiency in electrochemical water splitting (Li et al 2016). Similarly,Pt-based on noble metals does well in HER. The scarcity and high cost of noble metal-based catalysts are also the main factors limiting their widespread application. Due to their improved activity, low cost, and abundance, transition metal-based electrocatalysts have been used as an alternative for noble metal

catalysts for the past two decades. Layered double hydroxides, metal oxides, and metal nitrides are examples of transition metal-based electrocatalysts. For efficient electrochemical water splitting, chalcogenides and metal phosphides have been explored. Transition-metal oxides, especially cobalt-based, including CoO and Co_3O_4, with high OER activity, have gotten a lot of interest in recent years as long-lasting, inexpensive, and abundant electrocatalysts (Song et al 2018). To overcome this limitation, conducting carbon materials and highly porous carbon materials with large specific surface area (SSA), such as carbon nanotubes, graphene, and reduced graphene oxide (rGO), have been used to support such materials for the improvement of Co-based electrocatalysts by promoting metal/metal oxide@nanoparticales heterostructures(Jin et al 2015; Wang et al 2015; Tsutsumi et al 2017). In the hydrothermal approach, the current work belongs to a simple Co-based coordination polymerization with nitrilotriacetic acid (NTA) as the chelating ligand. The Co-NTA nanowires were employed as precursors for the Co@NC catalyst, which may be used to alter the catalytic activity of as-made Co-NTA for efficient OER by doping noble metal catalysts like palladium at a much lower ratio (Nishioka et al 2019).

Furthermore, the electrocatalytic activity can be increased by modifying the electrical structure through combination doping, oxygen-vacancy generation, and other methods. The catalysts' water adsorption ability and conductivity, dependent on electron delocalization and electronic configurations, are solely responsible for OER formation. The introduction of noble metal nanoparticles such as palladium may allow doping with chelating Co@NC catalyst at low ratios, potentially augmentation of catalytic activity by many orders of magnitude (Matsumoto et al 2021). As a result, they use functional palladium nanoparticles produced from organotrialkoxysilane to meet such requirements (Pandey et al 2014; Pandey et al 2016; Pandey et al 2015; Pandey et al 2018).

Organotrialkoxysilanes such as 3-aminopropyltrimethoxysilane,3-glycidoxypropyltrimethoxy- silane and 2-(3,4 epoxycyclohexyl)ethyltrimethoxysilane (EETMOS) have been proven to be effective functional materials for the rapid and regulated synthesis of noble metal nanoparticles (Tsutsumi et al 2017; Nishioka et al 2019; Matsumoto et al 2021; Pandey et al 2014; Pandey et al 2016).Controlled synthesis of Pd and Pd–Au nanoparticles: effect of organic amine and silanol groups on morphology and polycrystallinity of palladium nanoparticles have been demonstrated justifying the specific interaction between silanol residue and palladium nanoparticles with subsequent improvement in palladium nano geometry as a function of silica content(Pandey et al 2015). Accordingly, it is desirable to use functional organotrialkoxysilane to control the palladium nano geometry of as made Co@Pdnps bimetallic obtained after calcination that may significantly improve the catalytic evolution of oxygen in alkane media and is reported herein. Two systems of Co@Pdnps with variable silica contents are made, along with a third system made without silica to evaluate the impact of silica on OER. Indeed, fascinating findings on the effects of silica have been recorded, justifying (i) significant improvement in OER in the presence of silica as compared to that made without silica, (ii) the higher content of silica significantly improves the nano geometry of Co@Pdnps, and introduce effective interaction of bimetallic components during OER. One of the most fundamental and significant phenomena for the electrode/electrolyte interface is the electrochemically active surface area (ECSA). Both the supercapacitor electrode and the water splitting catalyst's ECSA, or the area of the electrode or catalyst that is open to the electrolyte for interaction, are very important components. These ECSA of the electrode may, in some circumstances, be a thousand times bigger than its geometric surface area. The active sites of the catalysts are where the electrochemical interactions, or charge storage and/or

transfer, take place. Therefore, higher ECSA leads in enhanced electrolyte ion accessibility to more electrochemically active sites, which enhances performance.The findings on these lines are reported in this article along with data recorded on XRD, XPS, Raman spectroscopy, and electrochemical oxygen evolution reactions using cyclic voltammetry, linear sweep voltammetry, Tafel plot, and impedance spectroscopy to justify the efficient catalytic property of a Co@Pdnps based catalyst. Here we have develop a cost-effective and stable Co-Pd nanoparticles catalyst which have a good catalytic efficiency per noble metal exhibiting an excellent OER activity in basic electrolytes, with a low overpotential at a high current density .

3.2. Results and Discussion

3.2.1 Synthesis and characterization of Co@Pdnps

The use of NTA as a chelating agent has been widely documented, and it may help generate a one-step cobalt NTA complex, which is a precursor to creating Co@NC, i.e., N-doped carbon most appropriate for controlled doping of organotrifunctionalized palladium nanoparticles. As a result, the initial step is to produce the Co-NTA, which will be used to fabricate Co@Pdnps in the future. SEM, TEM, and XRD confirm Co-NTA production, as illustrated in Figure-3.1. Figures 3.1a-b show SEM pictures of Co-NTA, whereas Figures 3.1c-d provide TEM images of Co-NTA, both of which support the rod-shaped nano-geometry of the as-made catalyst. The nanorod morphology of Co-NTA was revealed by scanning electron microscopic and transmission electron microscopic studies. Furthermore, as shown in Figure 3.1 e-f, the XRD and FTIR results confirm the production of Co-NTA. The appearance of a peak at 1682 cm^{-1} in the ATR-FTIR spectra of Co-NTA corresponded to the stretching frequency of the carbonyl functional group (Zheng et al 2015).The next step in the research is the synthesis of

Co@NC, which is necessary for doping EETMOS functionalized palladium nanoparticles Co@Pdnps.

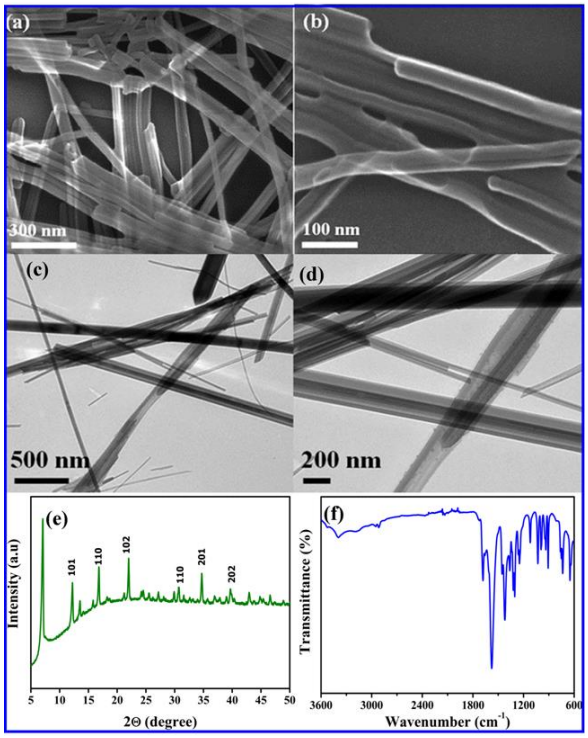

Figure 3.1 SEM image (a,b), TEM image (c,d), XRD (e) and FTIR (f) of Co-NTA

Co-NTA was pyrolyzed at 600^0C for 2 hours to produce Co@NC. TEM, XRD, XPS, SEM, IR, and Raman spectroscopy were used to characterize Co@NC, as indicated in Figure-3.2. The EDX result revealed the creation of Co@NC (Fig.3.2a) and related SEM pictures (Fig.3.2 b,c). The Raman spectroscopy of Co@NC, as shown in Fig.3.2d, confirms the creation of Co@NC, with peaks at 2700 cm^{-1}, 1583 cm^{-1}, and 1349 cm^{-1}, respectively, corresponding to 2D, G, and D bands of graphitic carbon, as demonstrated in Raman spectra (Fig.3.2d) (Wang et al 2019). Furthermore, as shown in Figure 3.2e, the XRD data offered a deeper understanding of the crystalline characteristics of the nanoparticle catalysts. The diffraction measurements for the Co@NC as demonstrated in Fig.3.2e further indicated that Co@NC formed in the same way as previously described (Su et al 2017). Co@NC is a combination of cubic (space group Fm3m, JCPDS No. 15-

0806)(Li et al 2010) and hexagonal (space group P63/mmc, JCPDS No. 05-0727) Co-phases(Pandey et al 2018). In Co@NC, the peak at 24^{o} corresponds to the (002) graphitic carbon plane (JCPDS No. 26-1076) (Zheng et al 2018).

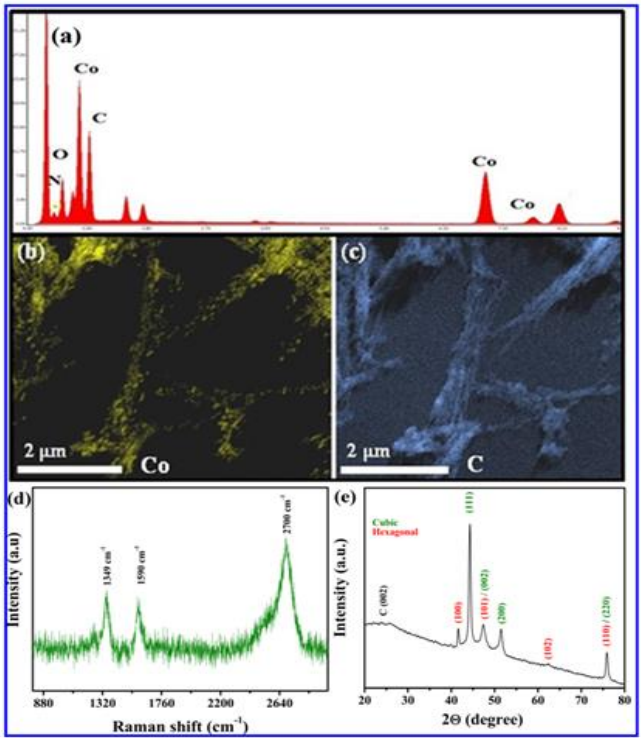

Figure 3.2. Energy dispersive x-ray analysis (a), SEM images (b,c), Raman spectroscopy (d) and XRD (e) of Co@NC

Figure 3.3a-d shows two different resolutions of TEM images of Co@NC, demonstrating the transformation of Co-rod-shaped NTA morphology to complexmorphology. Figure 3.3c displays an HRTEM picture of Co nanoparticles, showing that the lattice spacing of 0.20 nm corresponds to cubic Co's (111) plane (Rajabalee et al 1974). In figure 3.3 d The selected area electron diffraction (SAED) pattern revealed the crystalline nature of the core. The core-shell structure of the spherical nanoparticles with a Co core wrapped within an N-doped graphene shell was revealed by high-resolution TEM (HRTEM). The core was found to be a mixture of cubic (space group: Fm3m) and hexagonal (space group: P63/mmc) cobalt created by a helpful co-crystallization process. Finally, the

production of spherical nanoparticles with carbon nanofiber to form one-dimensional growth of the nanostructures by FE-SEM images of Co@NCas shown in Fig.3.3e-f.

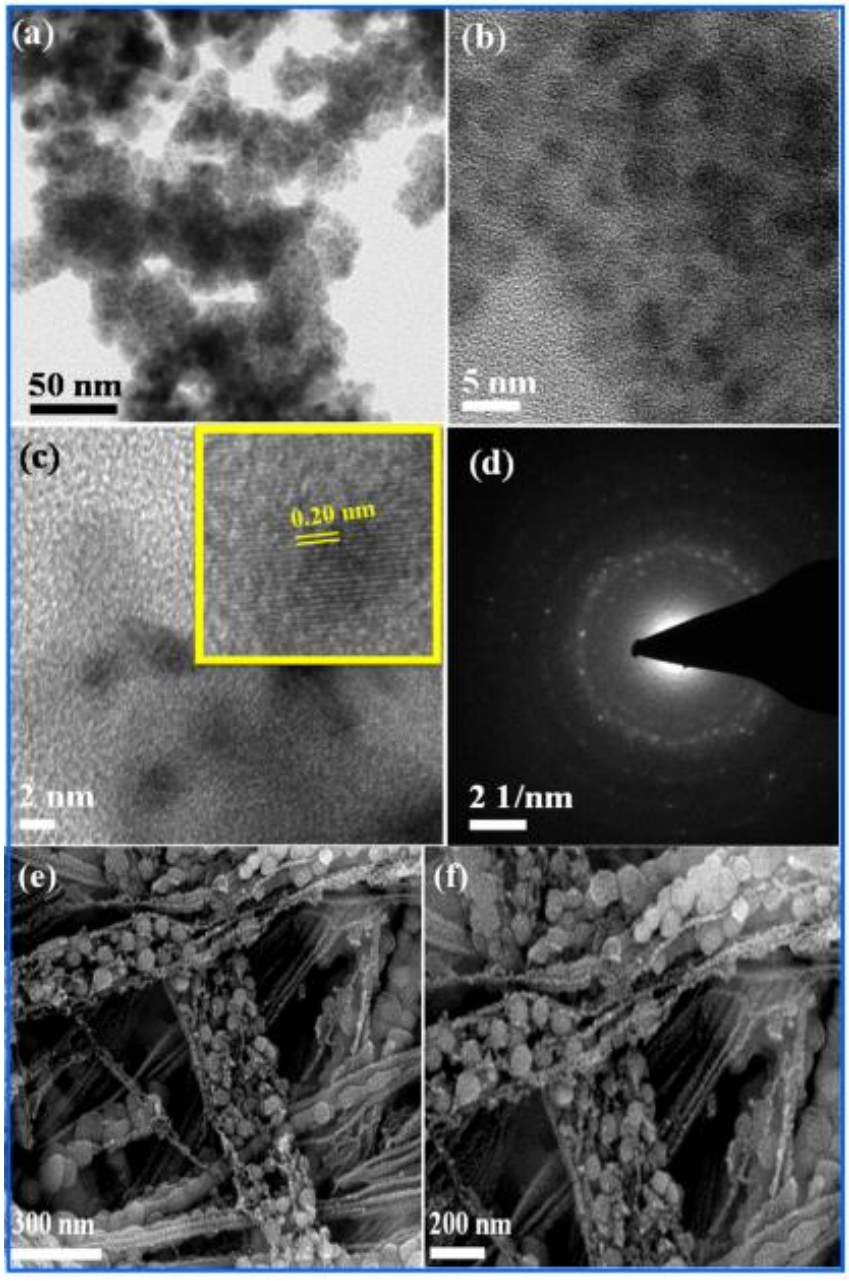

Figure 3.3 TEM images (a,b,c), SAED (d), SEM images (e,f) of Co@NC

The production of Co@Pdnps, which involves the functional activity of different content of silica and chelating cobalt precursors, is the next step of the present research. High-resolution scanning electron microscopy was used to examine the shape and size of the

as-made nanocatalyst (HR-SEM). HR-SEM pictures (Figure 3.4A, B) at two different magnification reveal the creation of bimetallic Co@Pdnps, whereas Fig 3.4B depicts the elemental mapping that supports the palladium content distribution in Co@Pdnps.

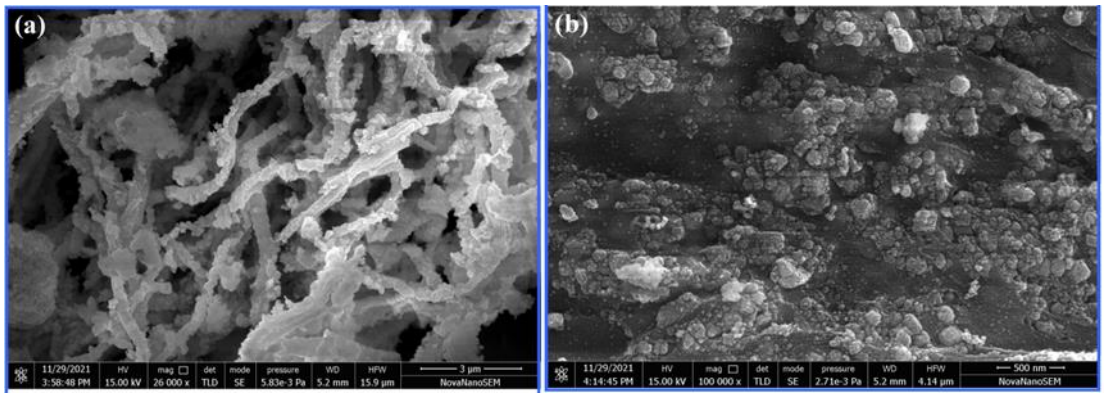

Figure3.4 A. SEM of Co@Pdnps1 at two different magnification

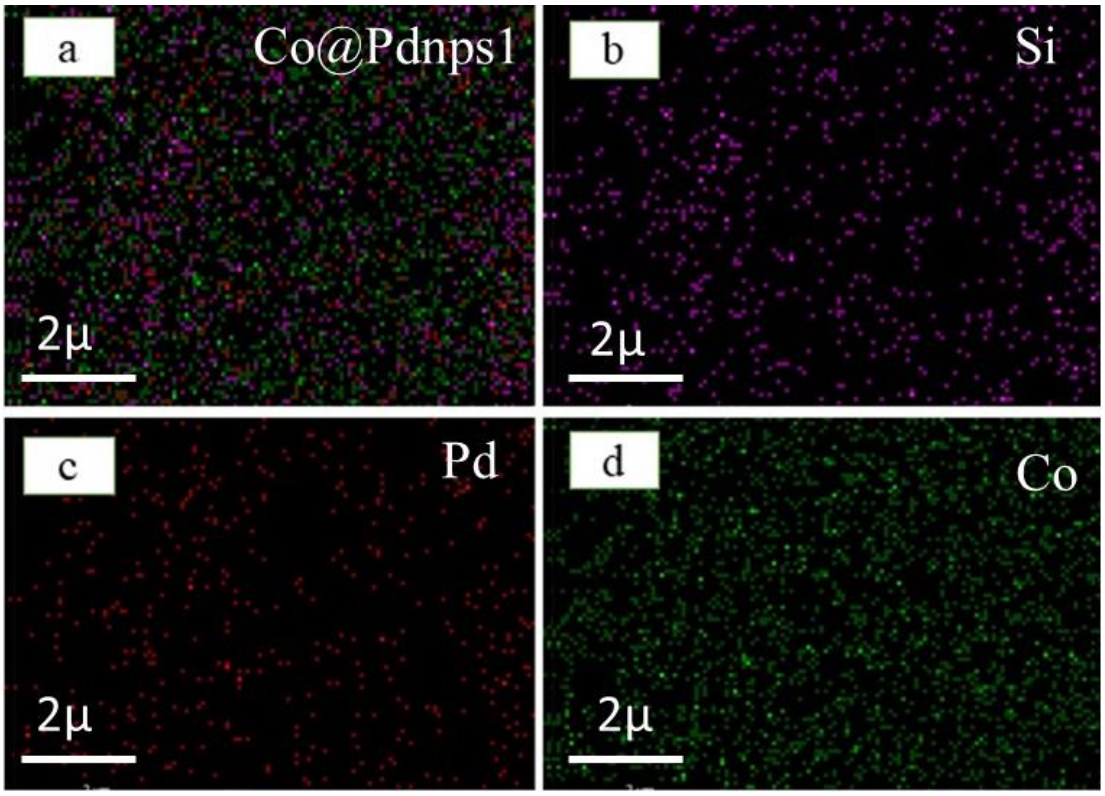

Figure 3.4B Elemental mapping of Co@Pdnps1

In Figure 3.5a, the surface atomic ratio of Co to Pd-nanoparticles shows 91% Co, 4% Si, and 4% Pd, which had the higher amount of Si as compared to figure 3.5b

(91.36%Co,2.81%Si,5.83%Pd) and figure 3.5c (90.52%Co,9.48%Pd) indicating that a Pd shell had covered the Co cores successfully.

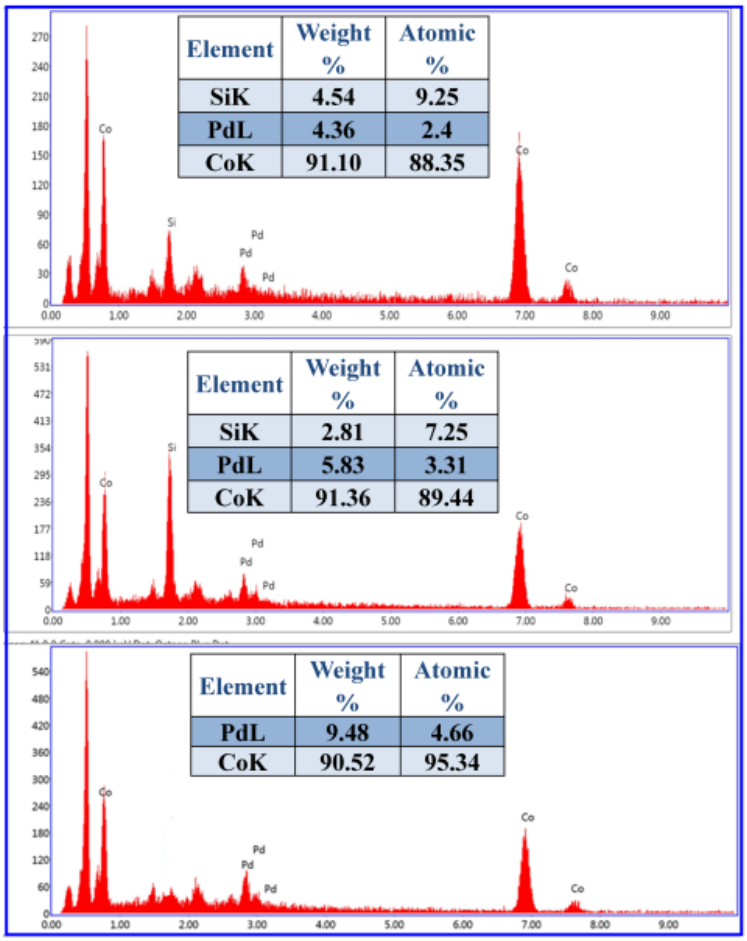

Figure 3.5 Energy dispersive x-ray analysis; Co@Pdnps1(a), Co@Pdnps2 (b), Co@Pdnps3 (c).

Its size is smaller than the other two. This difference is attributable to the type of electrical distribution used and changes in the two metals' external environments. The XRD pattern was used to index the selected region electron diffraction pattern, then indexed for cubic cobalt's (111) plane. Pd (200) nanoparticles are bimetallic nanoparticles. The average size of Pdnps1 and Pdnps3 is 8±2 nm and 25±5 nm, respectively, as shown in Fig 3.6. EETMOS, a moderate reducing agent that assures the reduction of Pd^{2+} ions, was used to make palladium nanoparticles. The synthesis of grey-black homogeneous Pdnps takes 10-15 minutes at ambient temperature followed by an oven incubation at 40°C. The epoxy component found in EETMOS molecules was

shown to be reactive with cations, allowing them to be converted to zero-valent species. Pdnps can operate as nucleation foci when doped over a bulk metal Co catalyst. The histogram picture of Pd-nanoparticles in fig.3.6a and c, which depicts the size of the Pdnps1 and Pdnps3, demonstrates the relevance of the alkoxysilane (EETMOS) in the nanoparticles'-controlled nucleation. The SAED patterns can be seen in the TEM images in Fig 3.6 b and d, which reveal the changes in crystallinity of the Pdnps1 and the Pdnps3.

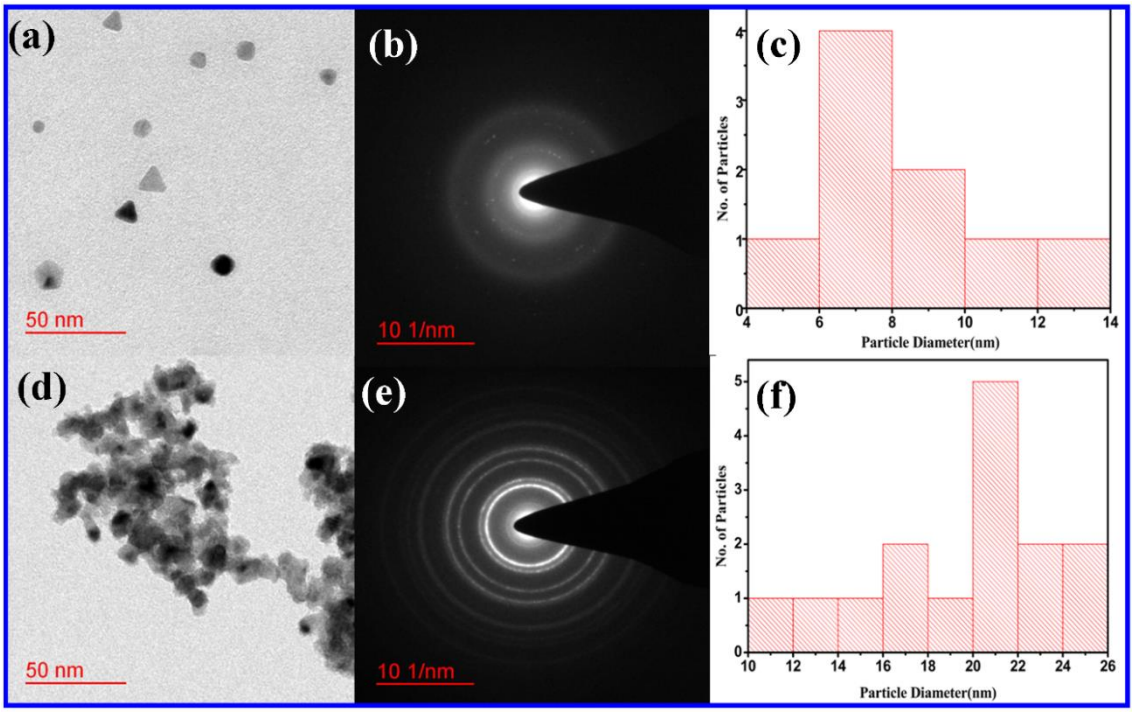

Figure 3.6. TEM images, SAED pattern and particles size distribution of Pdnps1 (a); (b); (c); Pdnps3 (d); (e); (f) respectively.

From Figure 3.7 (c,f and i), it is clear that the Co@Pdnps1,Co@Pdnps2 and Co@Pdnps3 particle sizes are 20±5 25±5 and 45±5nm, respectively. This difference in the nano geometry of particle size is due to the presence and absence of Si. Figure 3.7 (b,e and h) SAED pattern clear that crystallinity decrease when Si content increase. Figure 3.7 (a,d and g) displays an HRTEM picture of Co@Pdnps1,Co@Pdnps2 and Co@Pdnps3,demonstrating the lattice spacing of 0.21 nm and 1.4 nm.

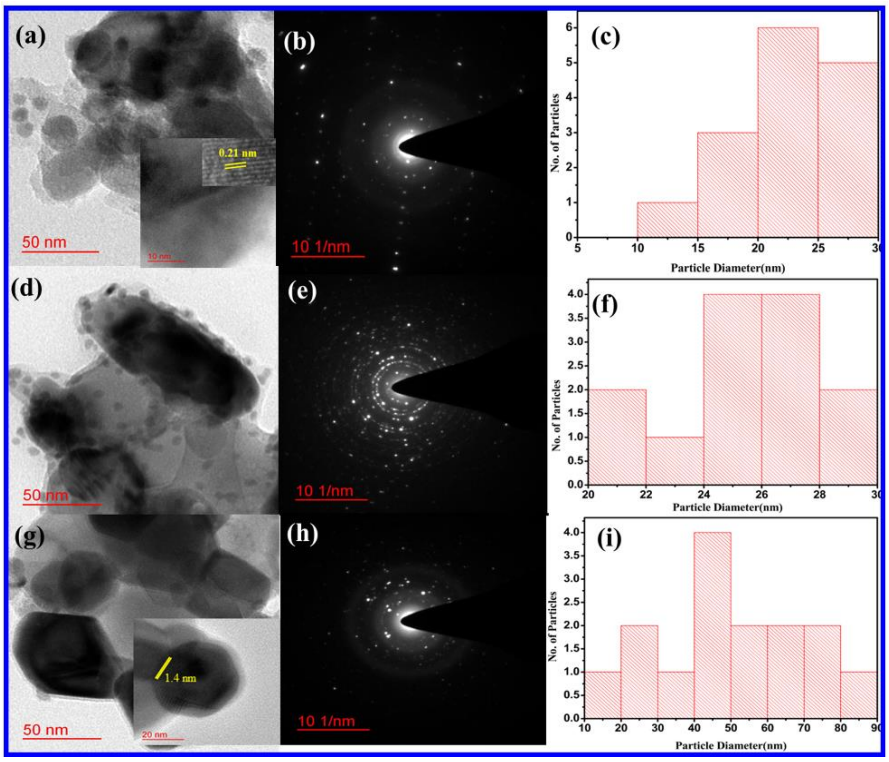

Figure 3.7. TEM image, SAED Pattern and particles size distribution of Co@Pdnps1(ab,c); Co@Pdnps2(d,e,f) and Co@Pdnps3(g,h,i) respectively.

Fig 3.8a-d shows X-ray photoelectron spectra of Co@NC, The Co 2p peak, was fragmented into two peaks, $2p_{3/2}$ and $2p_{1/2}$, with binding energies of 779.2 eV 795.0 eV, respectively (Zheng et al 2014). Metallic Co^0 was assigned a peak at 778.5 eV. The peak at 781.9 eV is originated from Co^{2+} owing to surface oxidation of Co^0, whereas the peak at 780.3 eV is originated from Co^{2+}(Jiang et al 2017; Guo et al 2018; Kumar et al 2013). N 1s XPS-spectrum was deconvoluted into four peaks The pyrrolic-N, graphitic-N oxidized-N, and pyridinic-N species had maxima at 400.0 eV, 401.9 eV, 405.1eV, and 398.1 eV, respectively(Jiang et al 2017; Guo et al 2018; Kumar et al 2013; Lee et al 2010). The C 1s XPS spectrum was fitted for the Peaks at 286.1 eV and 284.6 eV were given to C=O and C-C species, respectively, while the peak at 285.2 eV was assigned to the C-N bond(Jin et al 2015; Zheng et al 2014; Rajabalee et al 1974; Jiang et al 2017).

The four peaks in the O 1s spectrum were attributed to the presence of surface-OH and absorbed H_2O molecules was attributed to the peaks at 530.5 eV and 531.5 eV, respectively, while C=O and C-O-C species were assigned to the peaks at 532.4 eV and 533.2 eV, respectively (Jiang et al 2017; Guo et al 2018; Kumar et al 2013; Lee et al 2010). Figure 3.7 e-f shows what happens when palladium nanoparticles are doped. The Pd 3d XPS spectra of the Co@Pdnps band of the Pd composite clearly show two peaks of Pd $3d_{5/2}$ and $3d_{3/2}$ pairs of doublets; the doublet detected at about 335.3 and 340.6 eV corresponds to Pd in oxidation state zero (0), while the other doublet detected at about 336.8 and 342.2 eV corresponds to Pd^{2+} (Xie et al 1990). The presence of Pd^{2+} might be due to the metal Pd atoms on the Co@NC catalyst's surface being quickly oxidized to Pd oxide. This indicates that the Pd has manifested as a metallic form.

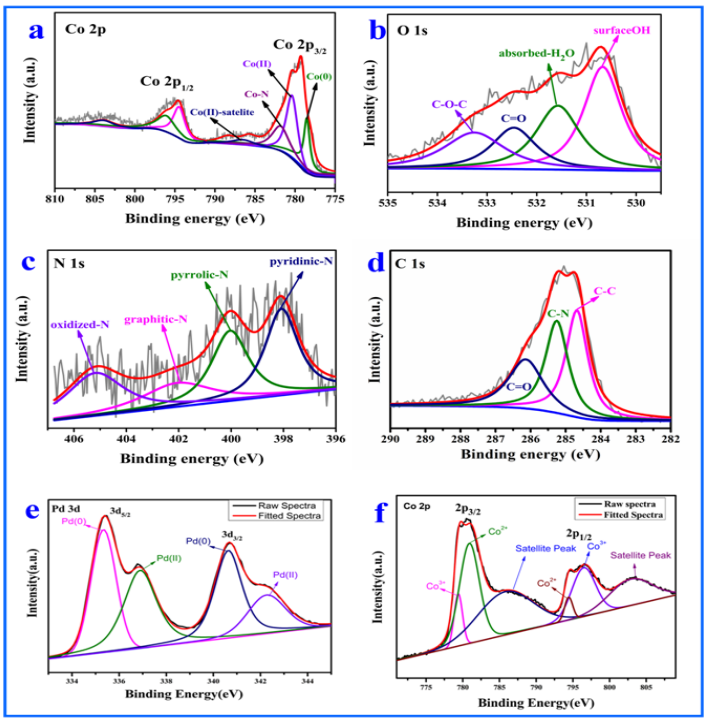

Figure 3.8 XPS analysis of Co@NC (a-d) and Co@Pdnps1 (e,f).

The movement of peak Pd^0 to lower values might be explained by the ultrafine size of the Pd nanoparticles shell and the enhanced electron-donating action from the inner Co atom

to the Pd atom. Figure 3.7 (a, d, and g) displays an HRTEM picture of Co@Pdnps1, Co@Pdnps2 and Co@Pdnps3, demonstrating the d-spacing value of 0.21 nm and 1.4 nm.

3.2.2 Electrochemistry of Co@NC and Co@Pdnps modified electrodes

Effect of nanostructured silica on OER functionalized organotrialkoxysilanes have been chosen for making Co@Pdnps1, Co@Pdnps2 this silanes namely allowed the efficient synthesis of Pdnps as discus above and subsequently calcinated at 700^0 C to eliminate Organic functionality link to silica residue, in addition, Pdnps made without silica has been used Co@Pdnp3 to understand the impact of silica on OER these three nanoparticles are tested for these catalytic activities in OER has been tested in below.To further understand the oxygen evolution reaction catalyzed by Co@NC and Co@Pdnps modified carbon cloth electrodes, researchers used linear sweep voltammetry, Tafel plots, electrochemical impedance spectroscopy, and cyclic voltammetry justifying significant advancement as compared to that of Pd-CoO system(Zhang et al 2016; Khan et al 2015) and Co inserted mesoporous silica (Lee et al 2010). Pd-CoO system was made from expensive CVD technology (Zhang et al 2016) and does not explore the role of silica whereas Pd-Co nanoparticles are synthetically inserted within mesoporous silica and does not serve the function of silica as potent stabilizer/binder for bimetallic nanocatalyst as nanostructured silica after calicination. Further the current finding further justify the role of nanostructured silica dependent OER justifying first report making potent and cheaper bimetallic nanocatalyst in OER. The findings on these lines are shown in Figure 3.9. The results of linear sweep voltammetry for bare CC, Co@NC, and Co@Pdnps modified electrodes in 1.0 M KOH solution at a scan rate of 10 mV s^{-1} are shown in Fig.3.9a. The raw Carbon cloth had minute electrocatalytic activity for OER. However, Co@NC and Co@Pdnps increased OER, with Co@Pdnps exhibiting substantial catalytic activity. Co@Pdnps1, Co@Pdnps2, Co@Pdnp3, and Co@NC modified electrodes, the

overpotentials corresponding to current density on the order of 5 mA/cm^{-2} are 0.85 V, 0.93V,0.86, and 1.00 V, respectively. Furthermore, the Co@Pdnps electrode has a much lower overpotential than the Co@NC electrode, indicating that the composite material has significantly improved OER catalytic activity over its single component.

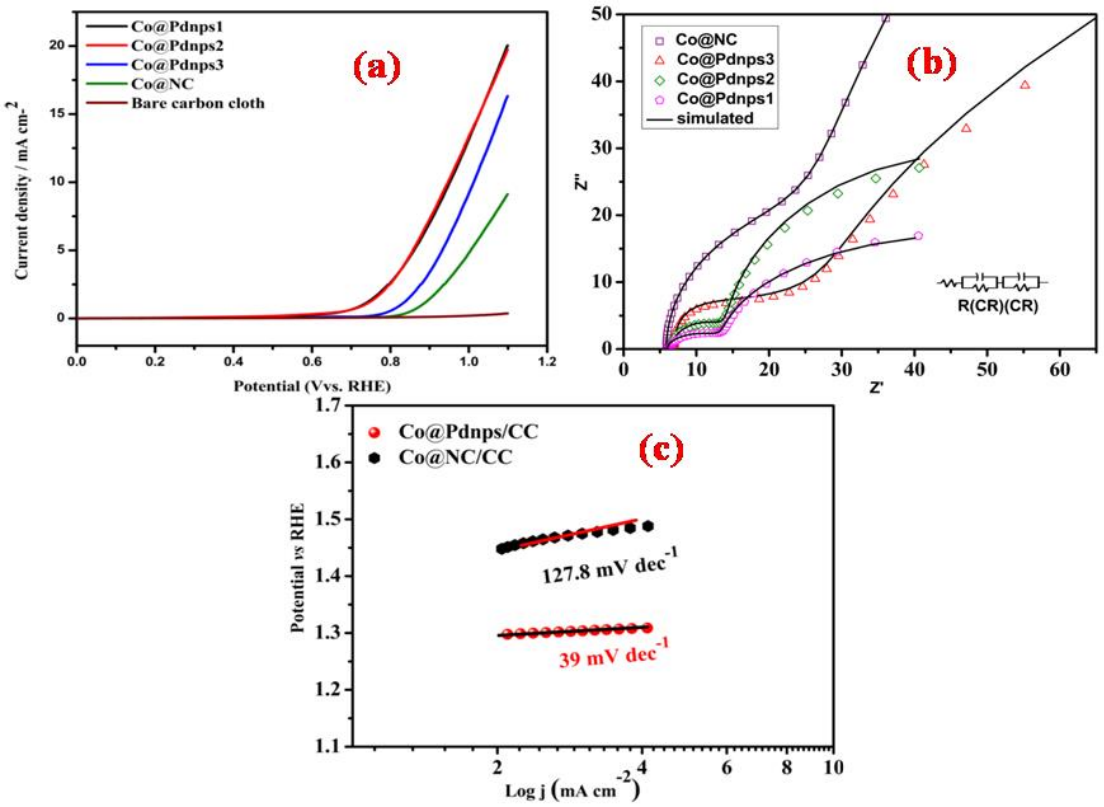

Figure 3.9 Linear sweep voltammetry (a), electrochemical impedance spectroscopy (b) and Tafel plot (c) of bare, Co@Pdnps2, Co@Pdnps2, Co@Pdnps3, and Co@NC modified electrodes.

The results show in Figure 3.9a from cyclic voltammetry of a blank CC, Co@NC, and Co@Pdnps modified electrode, demonstrating a several-fold increase in the catalytic activity of Co@Pdnps when palladium concentration is 4.3 percent in the cobalt-based heterogeneous catalyst. For further confirmation the ECSA study has been carried out. Equations (1) has been used, to get the primary surface parameters of the composite materials, that is ECSA. In order to calculate the ECSA using the double-layer capacitance technique, the CV data of all two composites as well as blank CC ,Co@NC

and Co@Pdnps were recorded in the newly created 1 M KOH electrolyte within a potential range of (1.03V - 1.12 V vs RHE) (Figure 9b). For the purpose of obtaining the double layer area, faster scan rates (5,10,15 and 20 mV s^{-1}) are used. We can determine the DLC (Cdl) of the composites, which is equal to the slope of the curve, from the scan rates vs. current density plot. The DLC are, respectively, 0.0013 F, 0.006 F and 0.0106 F for blank CC, Co@NC and Co@Pdnps. Since the redox-active sites directly affect the ECSA, it is predicted that Co@Pdnps would likely offer superior OER performance than other systems. ECSA calculate by using equation (1) are 32.5 cm^2, 150 cm^2 and 265 cm^2 for blank CC, Co@NC and Co@Pdnps respectively. Figure 3.9 (b) shows the electrochemical impedance spectroscopy (EIS) of a nanocatalystmodified electrode as it was manufactured. A semicircle section of the impedance spectra depicted in Figure 3.9b corresponds to charge transfer resistance, whereas a linear portion corresponds to diffusion-limited processes. The EIS of the Co@NC-modified electrode (Figure 3.9) revealed a virtually bigger semicircle diameter and a long straight line, indicating that in the case of Co@NC, the limiting diffusion phase of an electrochemical process. In including 4.3percent palladium in a bimetallic heterogeneous catalyst, the electron-transfer resistance (Ret), which is quite comparable to the semicircle diameter, is considerably lowered, supporting a significant improvement in catalytic activity for Co@Pdnps in OER.In the inset to Fig.3.9, an equivalent electric circuit is depicted. The fitting results were compared to the experimental data. To build the equivalent circuit, the solution resistance resistor (Rs) is connected with two parallel combinations of the resistor (R1 or Rct) and the constant phase element (CPE1 or CPE2).Figure 3.9(c) shows a Tafel plot that confirms the low slope value of 39mV/decade, showing the benefits of low palladium concentration in cobalt-based catalysts. Because of the functionality linked to the Cobalt precursor and the role of organotrialkoxysilane (EETMOS) in

making heterogeneous catalyst with several folds enhanced catalytic activity in OER, the successful construction of carbon cloth-supported Co@Pdnps nanoparticles promotes the electrocatalytic activity of a single component.

It is important to understand the exceptional catalytic application of as made cobalt and palladium nanoparticles embedded within silica matrix. The morphology of nanomaterials as shown in Figure 3.7 does not support the formation of bimetallic since Co@NC was made first through calcination followed by mixing organotrialkoxysilane stabilized palladium nanoparticles that hinder organized structure of Co and palladium clusters since palladium clusters are normally formed via organotrialkoxysilane mediated reduction of palladium cations(Pandey et al 2014; Pandey et al 2016). However after firing the mixture at 700^0C the cobalt and palladium components undergo effective binding within silica matrix rendering high stability of as made nanomaterial followed by closer interaction of these components during catalytic applications. We have been extending our work to study organized formation the bimetallic components via controlled synthesis and will be added subsequently. Nevertheless, it opens a new direction in making heterogeneous catalysts involving the advantage of organotrialkoxysilane. Finally, the video as shown in supporting information indicated the quick formation of oxygen during electrochemical water splitting https://youtu.be/TFw29jP-6nM, as well as the efficiency of the catalyst.

3.3 Conclusions

The recording result indicates the following significant finding (a)-Polycrystallinity decreases as a function of different content of silica, increased nano geometry Pd nanoparticle with an increase in silica concentration, which improves the rate of OER. (b)-In the presence of silica, Pdnps3 transitions from hexagonal to a circular and triangular shape.

The interaction of different forms of silica residue with as-synthesized Pd resulted in such diversity in polycrystalinity and microstructure of Pdnps.

After a seed-mediated growth event, Pd-doped bimetallic nanoparticles, known as Co@Pdnps, were created using a chemical reduction method. With a typical example of 2-(3,4epoxycyclohexyl)ethyltrimethoxysilane, the active activity of organotrialkoxysilane stabilized the nano-size bimetallic nanoparticles, unlike other Co@Pdnps catalysts. The sol-gel technique and steric stabilization afforded by EETMOS were used to regulate the nucleation of Pd nanoparticles on cobalt surfaces and promote increased nano geometry during pyrolysis, resulting in a several-fold increase in the heterogeneous catalyst's catalytic activity in OER. It is further confirm by the higher specific surface area in case of Co@Pdnps1, leads in enhanced electrolyte ion accessibility to more electrochemically active sites, which enhances performance. These nanoparticle catalysts are dominant bimetallic catalysts for the OER in alkaline environments, delivering a 5 mA cm^{-2} current density at an overpotential of Co@Pdnps1=0.85 V, Co@Pdnps2=0.93, Co@Pdnps3=0.86, and Co@NC=1.0 at an ideal loading of 3.5 mg/cm^2.Silica content and chelating Co@NC contributions to creating a heterogeneous catalyst for fast OER paved a new way.